Published in final edited form as:
Curr Biol. 2013 April 22; 23(8): 710–716. doi:10.1016/j.cub.2013.03.031.

Variation in the Dorsal gradient distribution is a source for modified scaling of germ layers in *Drosophila*

Juan Sebastian Chahda[1], **Rui Sousa-Neves**[2], and **Claudia Mieko Mizutani**[1,2,*]

[1]Department of Biology, Case Western Reserve University, Cleveland, OH, 44106, USA

[2]Department of Genetics and Genome Sciences, Case Western Reserve University, Cleveland, OH, 44106, USA

Abstract

Specification of germ layers along the dorso-ventral (DV) axis by morphogenetic gradients is an ideal model to study scaling properties of gradients and cell fate changes during evolution. Classical anatomical studies in divergent insects (e.g. flies and grasshopper) revealed that the neuroectodermal size is conserved and originates similar numbers of neuroblasts of homologous identity [1-3]. In contrast, mesodermal domains vary significantly in closely related *Drosophila* species [4]. To further investigate the underlying mechanisms of scaling of germ layers across *Drosophila* species, we quantified the Dorsal (Dl)/NFk-B gradient, the main morphogenetic gradient that initiates separation of the mesoderm, neuroectoderm and ectoderm [5-7]. We discovered a variable range of Toll activation across species and that Dl activates mesodermal genes at same threshold levels in *melanogaster* sibling species. We also show that the Dl gradient distribution can be modulated by nuclear size and packing densities. We propose that variation in mesodermal size occurs at a fast evolutionary rate and is an important mechanism to define the ventral boundary of the neuroectoderm.

RESULTS AND DISCUSSION

In *Drosophila*, a ventral-to-dorsal nuclear concentration gradient of maternal origin is established by the transport of Dl into the nuclei upon activation of Toll receptor [8-11]. Different Dl concentration levels turn on or off several target genes depending on their *cis*-regulatory sequences, which bind to Dl with different affinities (reviewed in [12]). Although the Dl regulatory network and characterization of *cis*-regulatory elements of target genes have been extensively studied [6], currently it is not known whether the shape and range of the Dl gradient itself vary across species and contribute to novel expression patterns. Different *Drosophila* species can have variations in egg size, total numbers of nuclei and packing densities [13-16], which are predicted to impact the formation of the Dl gradient.

To investigate these variables, we measured the embryonic DV diameter and total nuclei numbers distributed along the DV axis in *D. busckii* and *D. sechellia*, which have small and large egg sizes, respectively, and *D. melanogaster* and *D. simulans*, which have similar intermediate-sized eggs. The DV diameter increases 35% from small to intermediate eggs, and 15% from intermediate to large, while the nuclei vary from 84 to 101 (Table 1; Figure

*Corresponding author. claudiamieko@gmail.com. Phone: (216)368-1913. Fax: (216)342-1936.

1A). Since cleavage cycles are evolutionarily conserved [17,18], the variation in nuclei numbers likely arises from failed nuclei divisions, migration to the cortex and asymmetric packing distribution along the axes [14,19].

We next determined a set of measurements of the mesoderm in these species that included net numbers of DV nuclei expressing the mesodermal marker *sna* ("mesodermal nuclei"), the percentage of mesodermal nuclei in relation to all DV nuclei, and arc length distance. The latter measurement corresponds to the region occupied by the mesoderm in relation to the embryonic circumference and reports the range of peak Toll activation with highest Dl levels that activate *sna*. We found that the mesodermal nuclei in these species deviate significantly from the average 19 in *D. melanogaster* (Figure 1A; Table 1) [20-22]. In *D. melanogaster*, 21% of its DV nuclei are allocated to the mesoderm and occupy 21% arc length of the embryonic circumference. The percentages of mesodermal nuclei and arc length also match in *D. busckii* (17%). In contrast, *D. simulans* and *D. sechellia* have about 24% and 22% of mesodermal nuclei, respectively, but a mesodermal arc length of 27%. These results confirm and extend our previous results that the range of Toll signaling modify the absolute number of nuclei committed to the mesoderm in different species [4]. The discrepancy in percentages of mesodermal nuclei and arc length also corroborates previous findings that nuclei packing densities vary along the DV axis [14,19].

Cross-species comparison of nuclear Dorsal protein levels reveals gradients of different shapes

Next we quantified the Dl gradients in these species (Figure 1B, [23,24]). These data reveal striking variations in the distribution of Dl (Figure 1F-J. Individual graphs in Figure S1). *D. busckii* has the smallest mesoderm and sharpest gradient among all species, with highest Dl peak levels and steepest slope of the gradient. By fitting the normalized data to a Gaussian curve, we note a 19.3% decrease in full width at half maximum in the *D. busckii* curve in comparison to *D. melanogaster* (Figure 1J). In contrast, *D. simulans*, the species with highest percentage of mesodermal nuclei, also has the broadest gradient, with a shallow distribution of Dl levels corresponding to an increase of 22.7% in width compared to *D. melanogaster* (Figure 1J). Finally, *D. melanogaster* and *D. sechellia* have nearly identical gradient shapes (Figure 1G, I, J).

Mesodermal expansion does not rely on altered *sna* or twi sensitivity to Dl levels in sibling species

Since the normalization of the gradients is dimensionless, we could not distinguish whether the mesoderm is specified at similar or different Dl thresholds. To test whether the mesodermal span is influenced by either the Dl gradient shape or modified sensitivity of Dl target genes, we compared the Dl threshold levels required to activate the target genes *sna* and *twi* of sibling species in a single organism. We took advantage that *D. melanogaster, D. simulans* and *D. sechellia* hybridize to create hybrid embryos that receive maternal information solely from one species to establish the Dl gradient, and carry one autosomal copy of *sna* and *twi* genes from both species (Figure 2). We then visualized *sna* or *twi* nuclear nascent transcripts in hybrid embryos at the border of the mesoderm and neuroectoderm, and asked whether these nuclei responded to the same Dl threshold (i.e. presence of two nascent transcription dots) or different thresholds (i.e. presence of one dot).

Hybrid embryos from *D. melanogaster* mothers have a mesodermal size similar to the maternal species (Figure 2A, C) and two *sna* transcription dots at the boundary of the neuroectoderm (Figure 2E). Thus, the *sna* copy from *D. simulans* does not elicit a broader expression due to a higher sensitivity to Dl. To rule out differential *sna* activation due to divergence of Dl sequence, we analyzed hybrid embryos from the reverse cross with Dl

gradient from *D. simulans*. The same results were obtained, i.e. the mesodermal size is similar to the maternal species, and both *sna* nascent transcripts are activated in all mesodermal cells (Figure 2B, D, F). Identical results were obtained for *twi*, a direct Dl target (Figure S2A,B). Finally, forward and reverse hybrids between *D. melanogaster* and *D. sechellia* reveal same results (not shown).

Different gradients in the same scale of threshold levels reveal unique properties of scaling

When we transformed the Dl graphs to report actual levels required for *sna* activation in the sibling species (Figure 2G, see supplemental methods), two important features become apparent. First, the mesodermal expansion in *D. sechellia* is achieved by an absolute increase in Dl levels in comparison to *D. melanogaster*, which explains why the two species have different mesodermal domains despite their identical Dl gradient distribution. Second, the broadest mesodermal domain seen in *D. simulans* is consistent with its broader gradient compared to *D. melanogaster*. Thus, within a short divergence of 0.5 to 4.5 MYA that separate these three species [25], the Dl gradient acquired novel shapes and levels. These changes primarily affect the mesoderm, while in the neuroectoderm, Dl levels are very low and appear to equalize in these species (Figure 2G) without altering the expression domains of *sog* [4] or columnar neural identity genes (Figure S2, C-F). Thus, in all three sibling species, *sna* and *twi* have equal sensitivity to Dl, and the mesodermal size increase is exclusively caused by changes in the Dl gradient. Regarding the more divergent species *D. busckii*, which does not hybridize with *melanogaster* subgroup, the *sna* sensitivity to Dl remains to be tested.

The Dl gradient shape in *D. melanogaster* is sensitive to changes in nuclear size and packing

Although our cross-species comparisons and hybrid analyses show that species-specific ranges of Toll activation alone can explain the range of the Dl gradient, these species exhibit differences in nuclear size and packing [14], which might contribute to the final shape of the gradient. The nuclear diameters vary from 4 to 7 μm (Figure 3), significantly expanding the nuclear surface area from 50.2 μm^2 (*D. busckii*), 95 μm^2 (*D. simulans*), 113 μm^2 (*D. melanogaster*) to 153.9 μm^2 (*D. sechellia*). Additionally, *D. melanogaster* and *D. sechellia* have densely packed nuclei compared to *D. busckii*, while *D. simulans* has an intermediate packing density (Figure S3).

To isolate the effect of nuclear size and density over the Dl gradient formation, we analyzed *D. melanogaster* embryos with unaltered Toll signaling, but with altered nuclear size and densities. We used *sesame* (*ssm*) and *gynogenetic-2; gynogenetic-3* (*gyn-2; gyn-3*) mutants that generate haploid embryos (i.e. undergo one more nuclear division) and triploids (i.e. one less division), to change nuclei numbers, size and packing (Figure 4A-C) [26-28]. These zygotic mutations do not affect the maternal Toll pathway.

The net numbers of *sna+* mesodermal nuclei in haploids and triploids changes significantly. Haploids have on average 25 mesodermal nuclei, which is statistically greater than the wt *D. melanogaster* average, but similar to *D. sechellia* and *D. simulans*. Triploids have 15 mesodermal nuclei, similar to *D. busckii* (Figure 4A-C, tables 1-2). Despite net variations in mesodermal nuclei, the mesodermal nuclei percentage remains at 21%, which is characteristic of *D. melanogaster* species. Similarly, the percent arc length of mesodermal domain in haploids and triploids is equal to wild type *D. melanogaster* (not shown), which is expected and consistent with the unaltered maternal Toll pathway in these zygotic mutants.

The quantification of Dl gradients in ploidy mutants reveals significant alterations in the way Dl is distributed (Figure 4; Figure S1). In haploids, the Dl gradient becomes broader and with lower peak levels in the ventral midline, following a distribution analogous to that of *D. simulans*. In contrast, triploids show a similar profile to *D. busckii*, with sharper Dl distribution and higher peak levels than in the wt. Thus, physical changes in nuclei size and packing can reshape the Dl gradient and consequently modify the number of nuclei allocated to the mesoderm, even in the presence of invariable Toll signaling levels. Previous live imaging with Dl-GFP excludes the possibility that the Dl concentration is modulated by chromatin binding (e.g. addition of one genome copy from haploid, to diploid, to triploid), since Dl never accumulates in nuclei but instead transiently binds to and dissociates from chromatin in short intervals [29].

The effect of nuclei over gradient formation has been modeled as reversible traps and as localized sites for morphogen degradation [30,31]. A high nuclear density could divert Dl transport into the nucleus and flatten the gradient (e.g. *D. simulans* and haploids), whereas a low density would sharpen it (e.g *D. busckii* and triploids). A caveat is the constant gradient shape seen throughout the last nuclear divisions of *D. melanogaster* [23,24,29], when nuclear size decreases and density doubles at each cycle [31]. Two hypotheses could explain our findings. One possibility is that the Dl gradient shapes of haploids and triploids are altered from the onset of gradient formation, since these mutants start out with smaller or larger nuclei than the wild type. Alternatively, it is possible that subtle changes in the Dl gradient distribution in the wild type throughout nuclear divisions do exist, but are undetectable with current measurement methods. The behavior of the Dl gradient seen here in the mutants could be used in the future to test a computational model proposed for the Dl gradient, which relied on restricted parameters that best fit the final shape of the gradient, but discarded several possibilities for the dynamics of the gradient at early stages [23].

Fast evolution of the Dl gradient and maintenance of the neuroectoderm

Unlike the AP gradient of Bicoid that is scaled to size in divergent flies [15,18], the Dl gradient does not intrinsically scale. Indeed, distortions in mesodermal size are significantly higher than minor changes in the positioning of stripes of segmentation genes [14,16]. From an evolutionary standpoint, it is not entirely surprising the lack of co-evolution of *cis*-regulatory sequences of Dl targets, since the species studied here diverged very recently and did not have time to accumulate differences as noticeable as those of more distant lineages, such as *D. virilis* and *D. pseudoobscura* [32,33]. What is surprising is the change in several traits of DV diameter, nuclear size and density in a relatively short time. Our experiments with ploidy mutants indicate that nuclear size and density can effectively generate diverse shapes and intensities of the Dl gradient. Interestingly, these physical traits evolved fast in parallel to a second group of fast-evolving immune response genes [34-37], also shared by the Toll DV pathway. The changes in the Toll pathway and effect of nuclear size and density over Dl nuclear import can easily explain the variations in the range of Toll activation observed (Figure 1) and the diverse shapes and intensities of the Dl gradient in each *Drosophila* lineage (Figure 2).

We previously showed that the evolutionary expansions and retractions of the mesoderm do not modify the stereotyped array of somatic muscles [4], and as such these variations could be considered a neutral or non-adaptive trait. However, the present results indicate that the DV patterning system evolved to allow shifts in the neuroectodermal borders to new DV positions that preserve the width of the neuroectodermal domain, which is adaptive since the constancy of this domain is absolutely crucial for correct specification of neuronal lineages [38-40]. Therefore, the observed Dl gradient shapes and DV repositioning of neuroectodermal borders in *Drosophilids* are likely to have been selected over generations from a pool of individuals with modified range of Toll signaling, nuclear size and density.

The experiments with hybrids reveal that the underlying mechanism that controls mesodermal size and shifts the ventral neuroectodermal border involves exclusively a variation in the range of Toll activation and Dl gradient shape, and is not due to differential gene response. Thus, whenever the range of Dl distribution is changed, the mesodermal/neuroectodermal border acquires a new position. The shift in the ventral neuroectodermal border concomitantly repositions the dorsal neuroectodermal border in relation to the ventral midline, beyond which the Dl levels are insufficient to repress *decapentaplegic* (*dpp*)/BMP-4. The acquisition of a new upper limit of the neuroectoderm is supported by three independent lines of evidence. First, the hybrid experiments show that the sibling species have equal Dl levels at the mesodermal/neuroectodermal border, which are likely to have similar decay to low background levels within the neuroectoderm, as suggested in the transformed Dl graphs (Figure 2G). Second, consistent with comparative anatomical studies in insects [1-3], the neuroectodermal width remains constant in the species tested here, as shown previously [4] and in greater detail here (Figure S2). Finally, the *dpp+* nuclei numbers and gene expression subdomains within the ectoderm vary across species (Ambrosi and Chahda, unpublished data).

An interesting feature of Dpp/BMP signaling is its role in repressing neural genes in the ectoderm and forming an opposing dorsal-to-ventral gradient that helps pattern the neuroectoderm [41]. We speculate that the interaction of Dl and Dpp/BMP gradients represents a larger self-organizing system capable of responding to the rapid evolution of nuclear size, density and embryo size, by modifying the mesoderm while correctly assigning neuroectodermal DV fates (graphical abstract).

EXPERIMENTAL PROCEDURES

Fly stocks and genetic crosses

y w D. melanogaster was used as wild type. The following stocks from Drosophila Species Center (UCSD) were used: *D. busckii* (wildtype, 300-0081-23), *D. simulans* (wild type, 14021-0251-199) and *D. sechellia* (*zn* [1]*v* [1]*f* [1], 14021-0248.19). To obtain hybrid embryos, *y w D. melanogaster* females were crossed to either *D. simulans* or *D. sechellia* males. The reverse cross was done using the isogenized mutant line Santa Maria *D. melanogaster*, collected from natural population (Sousa-Neves, unpublished data). Santa Maria males can bypass sexual rejection of *D. simulans* and *D. sechellia* females. Scoring and confirmation of hybrid progeny are described in Supplemental data. Haploid and triploid embryos were generated using *w, ssm*[28,42] (a gift from James Erickson) and *gynogenetic-2; gynogenetic-3* (*gyn*) ([43] Bloomington Stock Center), respectively. Genetic schemes and genotyping of embryos (Fig. S4) are explained in Supplemental data.

Measurements of egg size, nuclear numbers, size and packing densities

Measurements of embryo size were obtained from intact [44] and sectioned embryos using a Confocal microscope (Zeiss LSM700, see supplemental data). For DV measurements of DV perimeter, nuclear counts and mesodermal arc-length, cross-sections of trunk regions of stained embryos for *sna* RNA and DAPI nuclear dye [45] were analyzed using Image J software. For nuclear size and packing calculation, early blastoderm stage embryos stained for *sna* mRNA and anti-Lamin were mounted longitudinally, and confocal optical slices were taken across the entire width of *sna+* ventral nuclei. Images of the optical slice corresponding to the center of nuclei were analyzed using Photoshop to calculate pixel densities of the space between nuclei (Fig. S3). Statistical analyses were performed using the PAST software (version 2.09, http://folk.uio.no/ohammer/past/). The data was compared using one-way ANOVA, followed by Tukey's test for pairwise comparison. The cutoff used for statistical significance was $p<0.05$.

Immunohistochemistry

Embryos were collected for 5-6hrs at 25° C in grape juice agar plates supplemented with yeast, or Noni fruit leather (for *D. sechellia*), fixed and processed for *in situ* and protein staining, as described in[45]. Probes against *sna* and *twi* were labeled with digoxigenin (DIG) (Roche). Primary antibodies and dilutions used were: Sheep anti-DIG (1: 1,000, Roche), mouse anti-Lamin (1:1,000, Iowa Hybridoma Bank), mouse anti-Dorsal (1:1,000, Iowa Hybridoma Bank, used for *D. melanogaster, D. simulans* and *D. sechellia* species) and Rabbit anti-Dorsal (1:2,000, a gift from Steve Wasserman, UCSD, used for *D. busckii*). Rabbit anti-Dorsal and mouse-anti-Dorsal antibodies provided identical results for *yw D. melanogaster* (data not shown). Secondary antibodies were used at 1:500 concentration: Donkey anti-Sheep Alexa 488, Donkey anti-Rabbit Alexa 555, Donkey anti-mouse Alexa 647 (Invitrogen). Nuclei were stained with DAPI (Invitrogen) at 300 nM for 15 min.

Quantification of the Dorsal gradient

Cross sections from trunk regions of stained embryos were cut using a micro knife (Roboz) or a 26 gauge 3/8″ needle[46]. Embryo slices were mounted in ProLong Gold antifade (Invitrogen) and cured for 24 hrs at room temperature prior to imaging in a Zeiss LSM700 Confocal. Gain and offset settings were adjusted to non-saturating levels spanning entire 12-bit dynamic range [19]. Images were exported to AxioVision 4.8 (Zeiss) for data analysis. Average fluorescent intensity levels were obtained from circles of 10 μm^2 centered on the 30 most ventral nuclei stained with DAPI and *sna*. To normalize the gradient, we used a modified version of a previously described Dorsal normalization method [23], in which the lowest fluorescent intensity was subtracted from each data point, and then each data point was divided by the sum of all the data points. To estimate width at half maximum values, Dl concentration graphs were fitted to a Gaussian curve, using curve fitting feature from Matlab. The curve fitting also confirmed the location of ventral midline at the ventral-most cell expressing *sna*. For details on methods used for normalization and transformation of Dl graphs based on threshold levels that activate *sna* and *twi*, see supplemental information.

Supplementary Material

Refer to Web version on PubMed Central for supplementary material.

Acknowledgments

We thank Mirela Belu for assistance and lab members for comments, James Erickson for the *ssm* stock, the Iowa Hybridoma Bank and Drosophila Species Center (UCSD) for reagents. This work was supported by National Science Foundation grant IOS-1051662 and startup funds provided by Case Western Reserve University to CMM, by National Institutes of Health grant 1R21EB016535-01 to CMM and RSN, and initially by NIH R01NS29870 to E Bier. JSC was supported by a GAANN fellowship from the US Department of Education grant number P200A090191 and the College of Arts and Sciences of Case Western Reserve University.

References

1. Doe CQ. Molecular markers for identified neuroblasts and ganglion mother cells in the Drosophila central nervous system. Development. 1992; 116:855–863. [PubMed: 1295739]
2. Thomas JB, Bastiani MJ, Bate M, Goodman CS. From grasshopper to Drosophila: a common plan for neuronal development. Nature. 1984; 310:203–207. [PubMed: 6462206]
3. Whitington P. Evolution of neural development in the arthropods. Seminars in Cell & Developmental Biology. 1996; 7:605–614.
4. Belu M, Mizutani CM. Variation in Mesoderm Specification across Drosophilids Is Compensated by Different Rates of Myoblast Fusion during Body Wall Musculature Development. PLoS ONE. 2011; 6:e28970. [PubMed: 22194964]

5. Hong J-W, Hendrix DA, Papatsenko D, Levine MS. How the Dorsal gradient works: insights from postgenome technologies. Proc Natl Acad Sci U S A. 2008; 105:20072–20076. [PubMed: 19104040]
6. Reeves GT, Stathopoulos A. Graded dorsal and differential gene regulation in the Drosophila embryo. Cold Spring Harb Perspect Biol. 2009; 1:a000836. [PubMed: 20066095]
7. Lynch JA, Roth S. The evolution of dorsal-ventral patterning mechanisms in insects. Genes Dev. 2011; 25:107–118. [PubMed: 21245164]
8. Roth S, Stein D, Nüsslein-Volhard C. A gradient of nuclear localization of the dorsal protein determines dorsoventral pattern in the Drosophila embryo. Cell. 1989; 59:1189–1202. [PubMed: 2688897]
9. Rushlow CA, Han K, Manley JL, Levine M. The graded distribution of the dorsal morphogen is initiated by selective nuclear transport in Drosophila. Cell. 1989; 59:1165–1177. [PubMed: 2598265]
10. Steward R, Zusman SB, Huang LH, Schedl P. The dorsal protein is distributed in a gradient in early Drosophila embryos. Cell. 1988; 55:487–495. [PubMed: 2460244]
11. Anderson KV, Bokla L, Nusslein-Volhard C. Establishment of dorsal-ventral polarity in the Drosophila embryo: the induction of polarity by the Toll gene product. Cell. 1985; 42:791–798. [PubMed: 3931919]
12. Stathopoulos A, Levine M. Dorsal gradient networks in the Drosophila embryo. Dev Biol. 2002; 246:57–67. [PubMed: 12027434]
13. Markow TA, Beall S, Matzkin LM. Egg size, embryonic development time and ovoviviparity in Drosophila species. J Evol Biol. 2009; 22:430–434. [PubMed: 19032497]
14. Fowlkes CC, Eckenrode KB, Bragdon MD, Meyer M, Wunderlich Z, et al. A Conserved Developmental Patterning Network Produces Quantitatively Different Output in Multiple Species of Drosophila. PLoS Genet. 2011; 7:e1002346. [PubMed: 22046143]
15. Gregor T, Bialek W, de Ruyter van Steveninck RR, Tank DW, Wieschaus EF. Diffusion and scaling during early embryonic pattern formation. Proc Natl Acad Sci U S A. 2005; 102:18403–18407. [PubMed: 16352710]
16. Lott SE, Kreitman M, Palsson A, Alekseeva E, Ludwig MZ. Canalization of segmentation and its evolution in Drosophila. Proc Natl Acad Sci U S A. 2007; 104:10926–10931. [PubMed: 17569783]
17. Baker J, Theurkauf WE, Schubiger G. Dynamic changes in microtubule configuration correlate with nuclear migration in the preblastoderm Drosophila embryo. J Cell Biol. 1993; 122:113–121. [PubMed: 8314839]
18. Gregor T, McGregor AP, Wieschaus EF. Shape and function of the Bicoid morphogen gradient in dipteran species with different sized embryos. Dev Biol. 2008; 316:350–358. [PubMed: 18328473]
19. Keranen SV, Fowlkes CC, Luengo Hendriks CL, Sudar D, Knowles DW, et al. Three-dimensional morphology and gene expression in the Drosophila blastoderm at cellular resolution II: dynamics. Genome Biol. 2006; 7:R124. [PubMed: 17184547]
20. McHale P, Mizutani CM, Kosman D, Mackay DL, Belu M, et al. Gene length may contribute to graded transcriptional responses in the Drosophila embryo. Dev Biol. 2011; 360:230–240. [PubMed: 21920356]
21. Fowlkes CC, Hendriks CLL, Keränen SVE, Weber GH, Rübel O, et al. A quantitative spatiotemporal atlas of gene expression in the Drosophila blastoderm. Cell. 2008; 133:364–374. Available:http://www.ncbi.nlm.nih.gov/pubmed/18423206. [PubMed: 18423206]
22. Ip YT, Park RE, Kosman D, Yazdanbakhsh K, Levine M. dorsal-twist interactions establish snail expression in the presumptive mesoderm of the Drosophila embryo. Genes Dev. 1992; 6:1518–1530. [PubMed: 1644293]
23. Kanodia JS, Rikhy R, Kim Y, Lund VK, DeLotto R, et al. Dynamics of the Dorsal morphogen gradient. Proc Natl Acad Sci U S A. 2009; 106:21707–21712. [PubMed: 19996178]
24. Liberman LM, Reeves GT, Stathopoulos A. Quantitative imaging of the Dorsal nuclear gradient reveals limitations to threshold-dependent patterning in Drosophila. Proc Natl Acad Sci U S A. 2009; 106:22317–22322. [PubMed: 20018754]

25. Tamura K, Subramanian S, Kumar S. Temporal patterns of fruit fly (Drosophila) evolution revealed by mutation clocks. Molecular biology and evolution. 2004; 21:36–44. [PubMed: 12949132]
26. Edgar BA, Kiehle CP, Schubiger G. Cell cycle control by the nucleo-cytoplasmic ratio in early Drosophila development. Cell. 1986; 44:365–372. [PubMed: 3080248]
27. Grosshans J, Muller HA, Wieschaus E. Control of cleavage cycles in Drosophila embryos by fruhstart. Dev Cell. 2003; 5:285–294. [PubMed: 12919679]
28. Erickson JW, Quintero JJ. Indirect effects of ploidy suggest X chromosome dose, not the X:A ratio, signals sex in Drosophila. PLoS Biol. 2007; 5:e332. [PubMed: 18162044]
29. DeLotto R, DeLotto Y, Steward R, Lippincott-Schwartz J. Nucleocytoplasmic shuttling mediates the dynamic maintenance of nuclear Dorsal levels during Drosophila embryogenesis. Development. 2007; 134:4233–4241. [PubMed: 17978003]
30. Coppey M, Boettiger AN, Berezhkovskii AM, Shvartsman SY. Nuclear trapping shapes the terminal gradient in the Drosophila embryo. Curr Biol. 2008; 18:915–919. [PubMed: 18571412]
31. Gregor T, Wieschaus EF, McGregor AP, Bialek W, Tank DW. Stability and nuclear dynamics of the bicoid morphogen gradient. Cell. 2007; 130:141–152. [PubMed: 17632061]
32. Crocker J, Tamori Y, Erives A. Evolution acts on enhancer organization to fine-tune gradient threshold readouts. PLoS Biol. 2008; 6:e263. [PubMed: 18986212]
33. Crocker J, Potter N, Erives A. Dynamic evolution of precise regulatory encodings creates the clustered site signature of enhancers. Nature communications. 2010; 1:99.
34. Clark AG, Eisen MB, Smith DR, Bergman CM, Oliver B, et al. Evolution of genes and genomes on the Drosophila phylogeny. Nature. 2007; 450:203–218. [PubMed: 17994087]
35. Jiggins FM, Kim KW. A screen for immunity genes evolving under positive selection in Drosophila. J Evol Biol. 2007; 20:965–970. [PubMed: 17465907]
36. Sousa-Neves R, Rosas A. An analysis of genetic changes during the divergence of Drosophila species. PloS one. 2010; 5:e10485. [PubMed: 20463966]
37. Obbard DJ, Welch JJ, Kim K-W, Jiggins FM. Quantifying adaptive evolution in the Drosophila immune system. PLoS genetics. 2009; 5:e1000698. [PubMed: 19851448]
38. McDonald JA, Holbrook S, Isshiki T, Weiss J, Doe CQ, et al. Dorsoventral patterning in the Drosophila central nervous system: the vnd homeobox gene specifies ventral column identity. Genes Dev. 1998; 12:3603–3612. [PubMed: 9832511]
39. Jimenez F, Martin-Morris LE, Velasco L, Chu H, Sierra J, et al. vnd, a gene required for early neurogenesis of Drosophila, encodes a homeodomain protein. EMBO J. 1995; 14:3487–3495. [PubMed: 7628450]
40. Weiss JB, Von Ohlen T, Mellerick DM, Dressler G, Doe CQ, et al. Dorsoventral patterning in the Drosophila central nervous system: the intermediate neuroblasts defective homeobox gene specifies intermediate column identity. Genes Dev. 1998; 12:3591–3602. [PubMed: 9832510]
41. Mizutani CM, Meyer N, Roelink H, Bier E. Threshold-dependent BMP-mediated repression: a model for a conserved mechanism that patterns the neuroectoderm. PLoS Biol. 2006; 4:e313. [PubMed: 16968133]
42. Loppin B, Docquier M, Bonneton F, Couble P. The maternal effect mutation sesame affects the formation of the male pronucleus in Drosophila melanogaster. Dev Biol. 2000; 222:392–404. [PubMed: 10837127]
43. Fuyama Y. Genetics of Parthenogenesis in DROSOPHILA MELANOGASTER. II. Characterization of a Gynogenetically Reproducing Strain. Genetics. 1986; 114:495–509. [PubMed: 17246347]
44. Belu M, Javier M, Ayasoufi K, Frischmann S, Jin C, et al. Upright imaging of Drosophila embryos. J Vis Exp. 2010; (43):e2175. DOI: 103791/2175 (2010).
45. Kosman D, Mizutani CM, Lemons D, Cox WG, McGinnis W, et al. Multiplex detection of RNA expression in Drosophila embryos. Science. 2004; 305:846. [PubMed: 15297669]
46. Grosshans J, Wieschaus E. A genetic link between morphogenesis and cell division during formation of the ventral furrow in Drosophila. Cell. 2000; 101:523–531. [PubMed: 10850494]

Highlights

- The germ layers of Drosophila species are unequally scaled to size during evolution.
- Evolutionary changes in nuclear size and density affect the Dl gradient scaling.
- Mesodermal variations rely on Dl distribution instead of regulation of target genes.
- Dl gradient distortions allow new positioning of ventral neuroectodermal border.

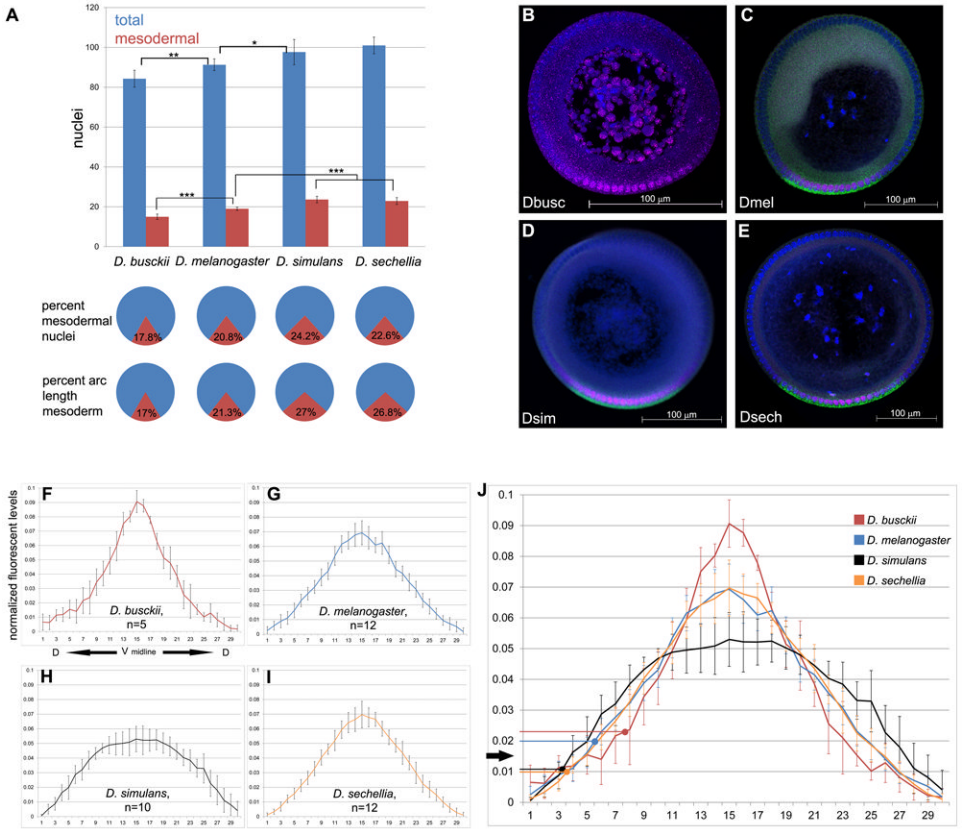

Figure 1. The distributions of nuclei, mesodermal domains and Dl levels changed across species

A) Histogram of average number of total nuclei (blue) and mesodermal nuclei (red) along the DV axis of blastoderm embryos. Bottom panel: pie charts with average percentage of nuclei that are mesodermal (red) and average percent of arc length corresponding to the mesoderm (red). Sample size for total nuclei counts are *D. busckii* n=12, *D. melanogaster* n=13, *D. simulans* n=17, *D. sechellia* n=13. Sample size for mesodermal nuclei: *D. busckii* n=13, *D. melanogaster* n=8, *D. simulans* n=11, *D. sechellia* n=10. Error bars are one standard deviation in both directions. Statistical significance (* = p<.05, ** = p<.01, *** = p<.001). (B-E) Blastoderm cross sections used for Dorsal gradient quantification, stained for Dorsal protein (magenta), *sna* mRNA (green, C-E) and DAPI nuclear dye (blue). B) *D. busckii* has the smallest embryo, followed by (B) *D. melanogaster*, (C) *D. simulans* and (D) *D. sechellia*. Ventral side is down. Scale bar: 100 µm. (F-J) Normalized graphs of average intensity levels of nuclear Dl protein (y-axis) per individual nucleus (x-axis). Graphs are centered on the ventral midline (x=15) based on *sna* expression domain, and extend dorsally from the center to the left (x=0) and right (x=30). (F) Average Dl distribution in *D. busckii* embryos (n=5). Note a sharper gradient with higher peak levels than *D. melanogaster* (G, n=12). In contrast, *D. simulans* Dl gradient (H, n=10) has a shallow profile, with lower peak levels and broader amplitude than *D. melanogaster*. (I) *D. sechellia* (n=12) gradient distribution is similar to *D. melanogaster*. J) Average distributions from all species combined onto one graph. Arrows indicate the Dl threshold levels for *sna* activation for the dorsal most *sna+* nuclei at the border of mesoderm and neuroectoderm. Error bars are one standard deviation in both directions. See also Figure S1.

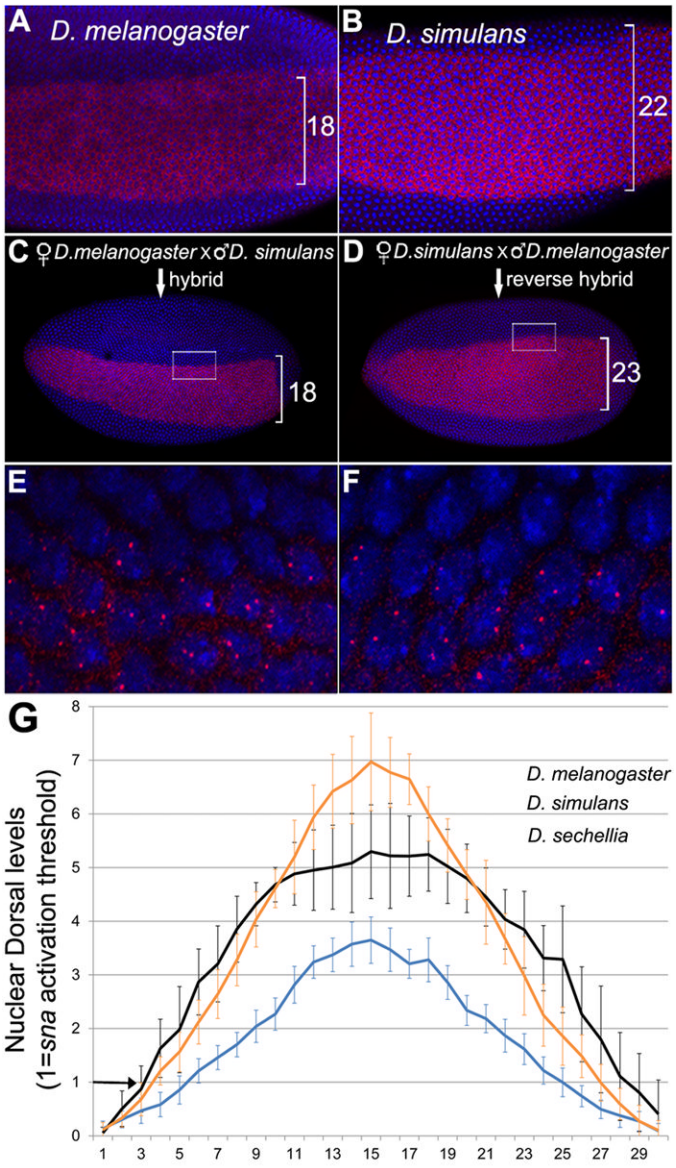

Figure 2. Sensitivity of mesodermal gene activation is identical among *D. melanogaster* sibling species

(A-D) Ventral view of whole mount blastoderm embryos stained for *sna* mRNA (red) and DAPI nuclear stain (blue). A) *D. melanogaster*. B) *D. simulans*. C) Hybrid embryo from *D. melanogaster* mother and *D. simulans* father. D) Hybrid embryo from *D. simulans* mother and *D. melanogaster* father. E, F) High magnification of boxed areas in C and D, respectively. Note the presence of two nuclear transcription dots per nucleus in cells along the border of *sna* expression, indicating that both copies of the *sna* gene from each species are activated. The abutting cells outside the mesoderm have both *sna* copies turned off. Similar results were obtained for *twi* (See Fig. S2) and hybrids between *D. sechellia* and *D. melanogaster* (not shown).

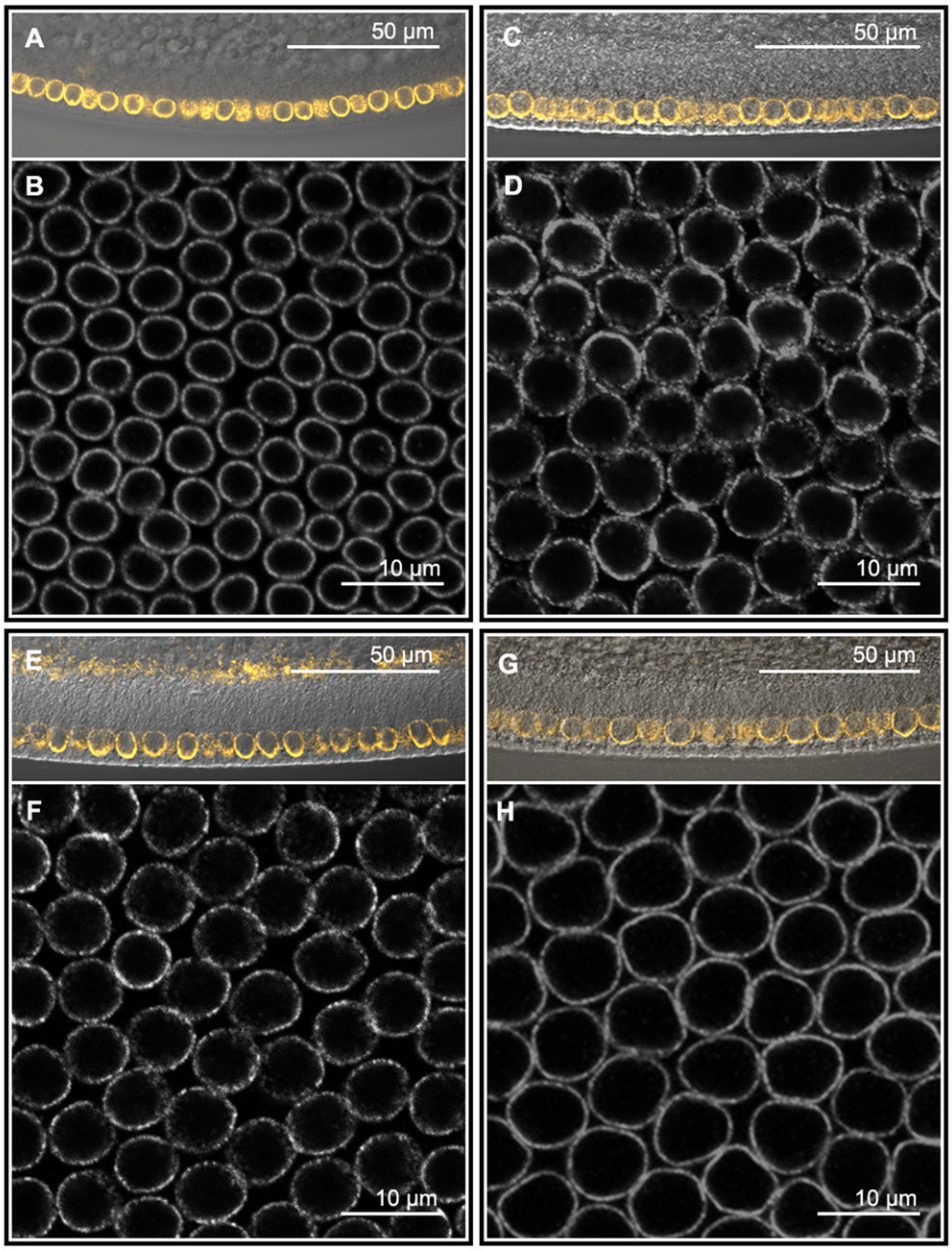

Figure 3. Drosophila species vary in nuclei size and densities

Anti-Lamin stainings of *D. busckii* (A, B), *D. melanogaster* (C, D), *D. simulans* (E, F) and *D. sechellia* (G, H) embryos. A, C, E, G) Sagittal view of embryos showing start of membrane growth using DIC transmitted light merged to Lamin staining (orange). B, D, F and H) Images of a single confocal plane corresponding to the center of nucleus were used to calculate average nuclear diameter, nuclear packing, and nuclear surface area (see Fig. S1 and methods). Ventral mesodermal nuclei of *D. busckii* (B) have the smallest size compared to the other species and the lowest density packing. D) *D. melanogaster* has nuclei slightly larger than (F) *D. simulans*. Nuclei of *D. sechellia* (H) have the largest size compared to the other species, and exhibit highest density packing along with *D. melanogaster*. Embryos were double stained for *sna* (not shown) to localize the ventral region from where the images were taken. See also figure S3.

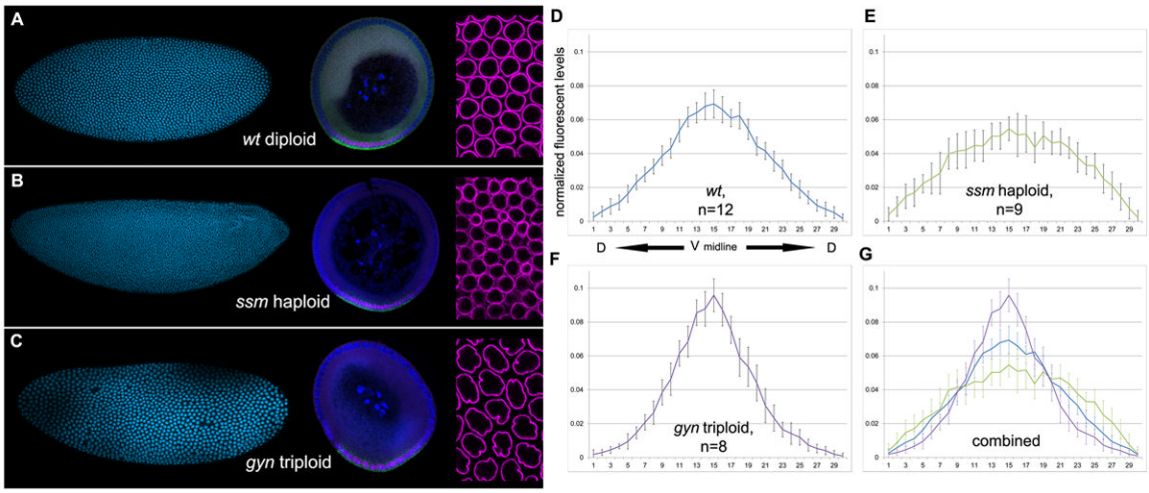

Figure 4. The Dl gradient is modified by nuclear size and packing density

(A-C) Whole mount blastoderm embryos (left) and corresponding cross-sections (middle) stained with DAPI nuclear dye (cyan, left), anti-Dorsal (magenta) and *sna* mRNA (green) of (A) *wt* D. melanogaster, (B) *ssm* and (C) *gyn* mutants. Right panel: Note increasing size in nuclei and density packing from haploid embryos (B), to diploids (A), to triploids (C) in anti-Lamin staining preparations (magenta). (D-G) Normalized graphs of average intensity levels of nuclear Dl protein (y-axis) per individual nucleus (x-axis). Graphs are centered on the ventral midline (x=15) and extend dorsally from the center to the left (x=0) and right (x=30). (D) Average Dl distribution of *wt D. melanogaster* (n=12), (E) haploid *ssm* mutants (n=9), and (F) triploid *gyn* mutants (n=8). (G) Average distributions were combined onto one graph. Wild type *D. melanogaster* (blue line), haploid *ssm* (green), and triploid *gyn* (purple). Error bars are one standard deviation in both directions. See also figure S4.

Table 1

Cross-species comparison of embryo size and DV nuclei

Means are given followed by standard deviations. n, sample size.

Species	Length	Diameter	Total DV nuclei	Mesodermal nuclei	Mesodermal percentage
D. busckii	378 μm (n=6)	186.8 μm (n=10)	84.3 ± 4.24 (n=12)	15 ± 1.35 (n=13)	18%
D. melanogaster	483 μm (n=6)	204.8 μm (n=7)	91.3 ± 2.95 (n=13)	19 ±.82 (n=8)	21%
D. simulans	472 μm (n=6)	205 μm (n=9)	97.6 ± 6.34 (n=17)	23.64 ± 1.63 (n=11)	24%
D. sechellia	573 μm (n=6)	269.7 μm (n=9)	101.3 ± 4.19 (n=13)	22.9 ± 1.73 (n=10)	23%

Table 2

DV nuclei in *D. melanogaster* wt, haploid and triploid mutants

Means are given followed by standard deviations. n, sample size.

Strain	Total nuclei	mesodermal nuclei
wt	91.3 ± 2.95 (n=13)	19 ± .82 (n=8)
ssm	115.92 ± 11.96 (n=12)	25.46 ± 3.73 (n=13)
gyn	67.67± 2.06 (n=6)	14.67 ± 1.86 (n=6)